The Influence of background state on the organization of Madden-Julian Oscillations

Lei Zhou Lamont-Dohery Earth Observatory, Columbia University
Raghu Murtugudde ESSIC/AOSC, University of Maryland
Richard Neale NCAR, Boulder, CO
Markus Jochum NCAR, Boulder, CO

Overview

Model: 1. CCSM3, a global climate model which fully couples the atmosphere, ocean, land, and sea ice;
2. Two modifications to the convection scheme:
a. Dilute plume approximation;
b. Convective momentum transport (CMT).

Conclusions:

1. The simulated intraseasonal variabilities (ISVs) become stronger, because the relation between temperature perturbation and convective heating is adjusted due to the dilute plume approximation;
2. Inclusion of CMT largely removes the easterly wind bias over the Indian Ocean and the maritime continent. As a result, the ISVs are better organized and the simulated MJOs with CMT are more realistic.

I. CCSM3 and modification to convection scheme

The atmospheric component has 26 vertical levels and a horizontal resolution of 1.9° latitude × 2.5° longitude.

There are 40 vertical levels in the ocean component with a nominal horizontal resolution of 1° × 1° .

The parameterization of the deep convection basically follows Zhang-McFarlane scheme.

Two modifications:

1. Dilute plume approximation. 2. Convective momentum transport.

Two fully coupled CCSM experiments were performed, one is the control run (C3OLD) without the above two changes while the other one includes the two modifications (C3NEW).

Both experiments are conducted for 102 years and the last 20 years (Years 83 – Year 102) provide the period of focus for the higher-frequency, daily output analysis.

II. Strength of simulated MJOs

1. Stronger ISVs in C3NEW

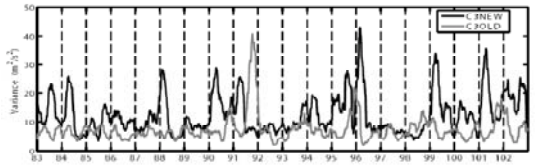

Figure 1 Variance of the intraseasonal zonal winds at 200 hPa averaged from 10° S to 10° N and from 50° E to 100° E and then passing a 101-day running mean.

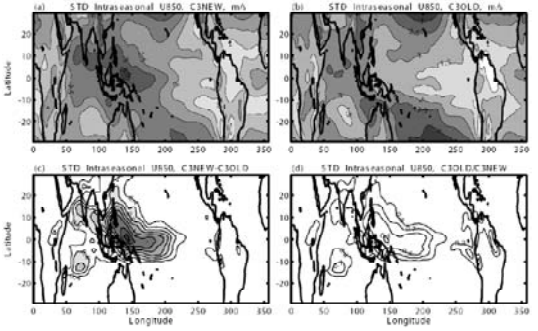

Figure 2 STDs of intraseasonal zonal winds at 850 hPa in C3NEW **(a)** and in C3OLD **(b)**. The differences and the ratios between the STDs in C3NEW and C3OLD are shown in **(c)** and **(d)**, respectively.

2. Adjusted relation between temperature perturbation and convective heating

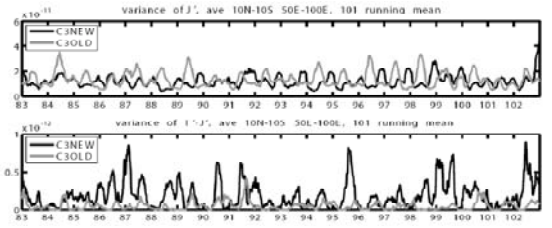

Figure 3 Variance of J' and $T'J'$ averaged in the vertical and within 10°S – 10°N and 50°E – 100°E, then passing a 101-day running mean. The unit for J' is K s^{-1} and the unit for $T'J'$ is K^2 s^{-1}.

III. Organization of simulated MJOs

1. Removal of easterly wind bias

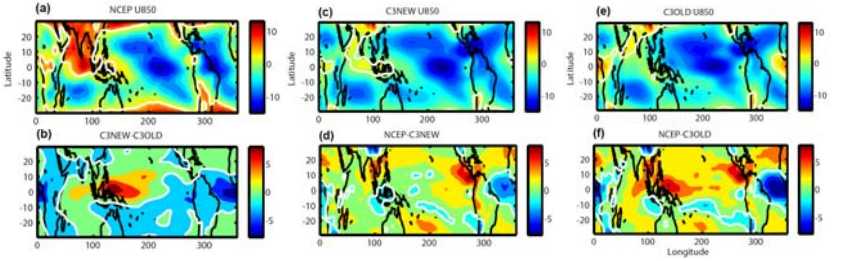

Figure 4 Mean zonal winds at 850 hPa in the NCEP reanalysis **(a)**, C3NEW **(c)**, and C3OLD **(e)**. Differences between C3NEW and C3OLD, between NCEP and C3NEW, between NCEP and C3OLD are shown in the right column. The unit is m s^{-1}.

2. Better organization in C3NEW

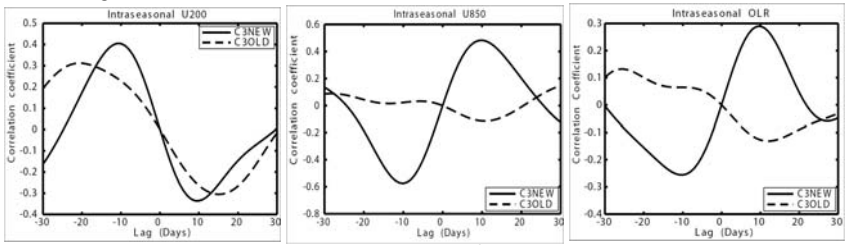

Figure 5 Cross-correlations between PC1 and PC2 of the intraseasonal variables.

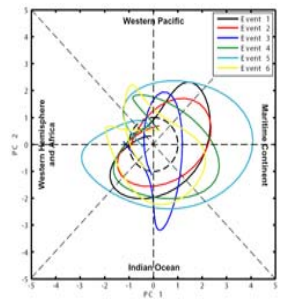

Figure 6 Phase diagram in terms of the first two PCs of the EOF analysis for 6 MJO events in C3NEW. Every curve rotates anti-clockwise. The dash cycle is the unit cycle.

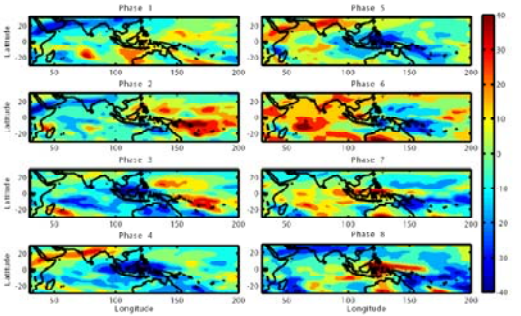

Figure 7 Composite intraseasonal OLR anomalies during 6 MJO events in C3NEW. The unit is W m^{-2}.

3. Influence of background westerly winds

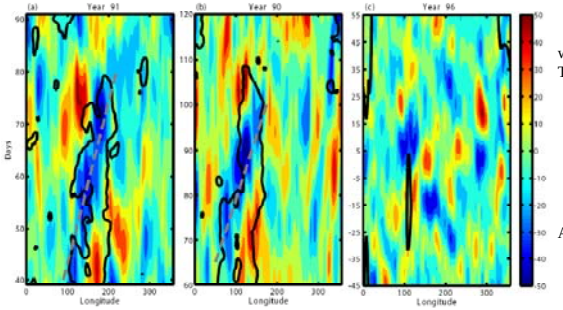

Figure 8 (a) and **(b)**: Intraseasonal OLR anomalies (color shades) averaged between 10° N and 10° S during two MJO events in C3NEW with a unit of W m^{-2}. The gray dash lines mark an eastward propagation speed of **4 m s^{-1}**. The black contours represent the background zonal winds of **4 m s^{-1}** in the same region. **(c)**: Intraseasonal OLR anomalies (color shades) averaged between 10° N and 10° S when the ISVs are strong in C3OLD. The black contours also represent the background zonal winds of **4 m s^{-1}** in the same region. **Similar figures can be shown with NCEP reanalysis.**

$$T'J' = T\int_0^\infty A(k)e^{i\psi t}dk \quad (1)$$

where $\psi = kU - \omega(k)$.

Then integration by parts yields

$$T'J' = T\int_0^\infty \frac{Ae^{i\psi t}}{d\psi/dk}d\psi$$

$$= \frac{T}{it}\frac{Ae^{i\psi t}}{d\psi/dk}\Big|_0^\infty - \frac{T}{it}\int_0^\infty e^{i\psi t}d\psi\frac{d}{d\psi}\left(\frac{A}{d\psi/dk}\right) \quad (2)$$

According to the method of stationary phase

$$\partial\psi/\partial k = 0$$

$$c_g = \partial\omega/\partial k = U$$

For more information, please contact Lei Zhou: lz2268@columbia.edu

Lamont-Doherty Earth Observatory
COLUMBIA UNIVERSITY | EARTH INSTITUTE